

# De-tuning a coupled Climate Ice Sheet Model to simulate the North American Ice Sheet at the Last Glacial Maximum

Gandy Niall<sup>1</sup>, Astfalck Lachlan C<sup>2</sup>, Gregoire Lauren J<sup>3</sup>, Ivanovic Ruza F<sup>3</sup>, Patterson Violet L<sup>3</sup>, Sherriff-Tadano Sam<sup>3</sup>, Smith Robin Stuart<sup>4</sup>, Williamson Danny<sup>5</sup>, and Rigby Richard<sup>3</sup>

<sup>1</sup>Sheffield Hallam University

<sup>2</sup>School of Physics, Mathematics and Computing, The University of Western Australia

<sup>3</sup>University of Leeds

<sup>4</sup>University of Reading

<sup>5</sup>University of Exeter

November 16, 2022

## Abstract

The maximum extent of the last North American ice sheet is well constrained empirically, but it has proven to be challenging to simulate with coupled Climate-Ice Sheet models. Coupled Climate-Ice Sheet models are often too computationally expensive to sufficiently explore uncertainty in input parameters, and it is unlikely values calibrated to reproduce modern ice sheets will reproduce the known extent of the ice at the Last Glacial Maximum. To address this, we run a series of ensembles with a coupled Climate-Ice Sheet model (FAMOUS-ice), simulating the final stages of growth of the last North American Ice Sheets' maximum extent. Using this large ensemble approach, we explore the influence of uncertain ice sheet, albedo, atmospheric, and oceanic parameters on the ice sheet extent. We find that albedo parameters determine the majority of uncertainty when simulating the Last Glacial Maximum North American Ice Sheets. Importantly, different albedo parameters are needed to produce a good match to the Last Glacial Maximum North American Ice Sheets than have previously been used to model the contemporary Greenland Ice Sheet, due to differences in cloud cover over ablation zones. Thus calibrating coupled climate-ice sheet models solely for present day strongly biases simulations of past and future climates different from today.

## Hosted file

detuning\_laurentide\_supplement.docx available at <https://authorea.com/users/524165/articles/595407-de-tuning-a-coupled-climate-ice-sheet-model-to-simulate-the-north-american-ice-sheet-at-the-last-glacial-maximum>

1           **De-tuning a coupled Climate Ice Sheet Model to**  
2           **simulate the North American Ice Sheet at the Last**  
3           **Glacial Maximum**

4           **N. Gandy<sup>1,2</sup>, L. C. Astfalck<sup>3,2</sup>, L. J. Gregoire<sup>2</sup>, R. F. Ivanovic<sup>2</sup>, V. L.**  
5           **Patterson<sup>2</sup>, S. Sherriff-Tadano<sup>2</sup>, R. S. Smith<sup>4</sup>, D. Williamson<sup>5,6</sup>, R. Rigby<sup>2,7</sup>**

6                           <sup>1</sup>Department of Natural and Built Environment, Sheffield Hallam University, UK

7                           <sup>2</sup>School of Earth and Environment, The University of Leeds, UK

8                           <sup>3</sup>School of Physics, Mathematics and Computing, The University of Western Australia, Australia

9                           <sup>4</sup>NCAS, Department of Meteorology, University of Reading, Reading, UK

10                           <sup>5</sup>Exeter University, UK

11                           <sup>6</sup>The Alan Turing Institute, UK

12                           <sup>7</sup>Centre for Environmental Modelling and Computation, University of Leeds, Leeds, UK

13           **Key Points:**

- 14           • Simulating the Last Glacial Maximum Laurentide Ice Sheet with the coupled Climate-  
15           Ice Sheet model FAMOUS-ice requires re-tuning
- 16           • We efficiently rule out unsuitable parameter values using a Gaussian Process em-  
17           ulator to design waves of short and long simulations
- 18           • The different cloud cover between North America and Greenland makes the Last  
19           Glacial Maximum a good test for climate-ice-sheet models

---

Corresponding author: Niall Gandy, [n.gandy@shu.ac.uk](mailto:n.gandy@shu.ac.uk)

## Abstract

The maximum extent of the last North American ice sheet is well constrained empirically, but it has proven to be challenging to simulate with coupled Climate-Ice Sheet models. Coupled Climate-Ice Sheet models are often too computationally expensive to sufficiently explore uncertainty in input parameters, and it is unlikely values calibrated to reproduce modern ice sheets will reproduce the known extent of the ice at the Last Glacial Maximum. To address this, we run a series of ensembles with a coupled Climate-Ice Sheet model (FAMOUS-ice), simulating the final stages of growth of the last North American Ice Sheets' maximum extent. Using this large ensemble approach, we explore the influence of uncertain ice sheet, albedo, atmospheric, and oceanic parameters on the ice sheet extent. We find that albedo parameters determine the majority of uncertainty when simulating the Last Glacial Maximum North American Ice Sheets. Importantly, different albedo parameters are needed to produce a good match to the Last Glacial Maximum North American Ice Sheets than have previously been used to model the contemporary Greenland Ice Sheet, due to differences in cloud cover over ablation zones. Thus calibrating coupled climate-ice sheet models solely for present day strongly biases simulations of past and future climates different from today.

## Plain Language Summary

At the peak of the last ice age, an ice sheet covered much of North America. The extent of this ice sheet is well-understood after decades of intensive data collection, but producing a computer simulation of the ice sheet which matches our observations has been a challenge. This is partly because of uncertainty about the “correct” model set-up to create the best simulation, and partly because the computer models used in the simulations require large computing resources.

In this paper, we present a series of simulations of the North American ice sheet at the peak of the last ice age using a fast-running computer model in which the atmosphere and ice sheets interact. We run hundreds of simulations to tackle the uncertainty about the optimum values for unknown input parameters. We find that the model's representation of how reflective the ice sheet surface is has the most impact on the size and shape of the simulated ice sheet. Importantly, the parameter values that produce the best simulations of modern-day Greenland produce poor simulations of the North American ice sheets during the last ice age, calling into question whether the parameters chosen for modern Greenland will produce reasonable simulations of future ice sheet change and sea level rise.

## 1 Introduction

Accurately estimating future changes in ice sheets is crucial for producing meaningful projections of future sea level rise (IPCC, 2021). Ice sheets interact with the atmosphere and ocean, and are vulnerable to instabilities in their growth and retreat (e.g. Shepherd et al., 2012; J. Gregory et al., 2012). These instabilities, along with the uncertainties in processes of climate and ice sheet evolution, make future projections using numerical models difficult, and the accuracy of any future simulations is a challenge to assess. For the Greenland ice sheet, one of the main sources of uncertainty is the future changes in surface mass balance (the balance of accumulation and melt of snow and ice at the surface) (Fettweis et al., 2011). This surface mass balance is highly dependent on both the climate and the ice sheet topography, as well as the strong interactions between the two. Thus projections of future Greenland evolution need to account for climate-ice sheet interactions (Goelzer et al., 2017). However, there are major challenges in representing surface mass balance and climate ice sheet interactions in models: (i) climate models often have large biases in ice sheet regions (Davy & Outten, 2020), (ii) these re-

69 regions are difficult environments to work in, limiting the observations we have of the cli-  
70 mate and surface mass balance (Vernon et al., 2013) and (iii) surface melt occurs in nar-  
71 row steep regions at the edge of the ice sheets that are difficult processes to capture or  
72 represent in global climate models.

73 Major progress has been made to tackle these challenges and there are now sev-  
74 eral earth system models that include interactive ice sheets in Greenland and/or Antarc-  
75 tica (e.g. Danabasoglu et al., 2020; R. S. Smith et al., 2021). However, there are numer-  
76 ous challenges in simulating climate-ice sheet interactions. Perhaps most acutely, there  
77 is a mismatch of spatial and temporal scales between typical ice sheet and global climate  
78 models. Spatially, kilometer (or sub-kilometer) processes are important for accurate sim-  
79 ulation of ice sheet processes, such as grounding line migration, and margin precipita-  
80 tion gradients (Franco et al., 2012; Cornford et al., 2013), so recent ice sheet models have  
81 been developed to simulate ice sheets at this scale, e.g. through adaptive mesh refine-  
82 ment, and they require climate (or surface mass balance inputs) at that scale. On the  
83 other hand, Atmosphere Ocean General Circulation Models (AOGCMs) have a grid-box  
84 size  $10\text{-}1000\times$  larger than the scale of modelled ice sheet processes and inputs (Sellar et  
85 al., 2019; Danabasoglu et al., 2020). This conundrum of mistmatching scales is flipped  
86 in the time domain. Temporally, AOGCMs require sub-daily timesteps to accurately sim-  
87 ulate the climate system, while ice sheet change is usually a multi-centennial process.  
88 The spatial-temporal mismatch of scales creates a problem for computational efficiency,  
89 since high resolution is needed for both and isn't easily compromised for one in favour  
90 of the other. Consequently, most AOGCMs cannot practically simulate interactive ice  
91 sheet change, instead prescribing the ice sheet extent as a boundary condition (e.g. Kageyama  
92 et al., 2017; Ivanovic et al., 2015; Menviel et al., 2019) and updating the ice sheet pe-  
93 riodically for palaeo runs where significant ice sheet change occurs. Similarly, ice sheet  
94 simulations often rely on prescribed climate or surface mass balance fields (e.g. L. J. Gre-  
95 goire et al., 2016; Patton et al., 2013; Gandy et al., 2021).

96 Nonetheless, recent technical advances have allowed coupled simulations of the cli-  
97 mate and ice sheets, through a combination of model development and increasing com-  
98 pute power. The spatial mismatch between ice sheet and climate model grids can be ad-  
99 dressed by calculating ice-sheet relevant processes, such as albedo calculations, with sub-  
100 gridscale parameterisations (Ganopolski et al., 2010; Vizcaíno et al., 2013; Ziemen et al.,  
101 2014; R. S. Smith et al., 2020, 2021). One way to solve the problem of time scale (sub-  
102 daily timesteps for multimillennial integrations) is to couple the ice sheet to climate mod-  
103 els which are typically computationally efficient, in part due to having relatively low spa-  
104 tial resolution, meaning the the simulations can be run for the length of time needed to  
105 spin-up and simulate the co-evolution of ice sheets and climate.

106 A remaining challenge is how coupled climate-ice sheet models should be calibrated  
107 and tested. For many models, uncertain parameters are hand-tuned to produce stable  
108 modern ice sheets of the right shape and size compared to observations. However, this  
109 only represents one point in time. The recent past, for which we have direct observations  
110 of ice sheets has seen relatively small changes compared to those expected in the next  
111 centuries. These observations thus provide poor constraints on the strength of climate-  
112 ice sheet feedbacks and there is a danger of over-fitting the model to modern conditions  
113 and compensating for biases in the simulated climate. To have confidence in the abil-  
114 ity of coupled climate-ice sheet models we need to test them under conditions different  
115 from today where we have sufficient observational constraints on the climate and ice sheets.

116 We propose to use the Last Glacial Maximum as a benchmark for coupled climate-  
117 ice sheet models. This period, which occurred around 21,000 years ago, has been a fo-  
118 cus of the Palaeoclimate Model Intercomparison Project since the 1990s (Kageyama, Abe-  
119 Ouchi, et al., 2021), because it was a period of relatively stable and well documented cli-  
120 mate, with CO<sub>2</sub> concentrations much lower than today (180 ppm). The North Amer-  
121 ican ice sheet is thought to have reached a relatively stable maximum extent, that is very

122 well reconstructed (e.g. Dyke et al., 2002; Peltier et al., 2015; Gowan et al., 2021). It is  
 123 thus possible to run equilibrium simulations under LGM conditions with an interactive  
 124 North American ice sheet until a stable maximum ice extent is reached, which can be  
 125 meaningfully compared to reconstructions. Ice at the LGM reached much lower latitudes  
 126 than today, providing a way to test the ability of models to represent SMB and climate-  
 127 ice interactions under energy balance conditions different than modern Greenland.

128 We use FAMOUS-Ice (R. S. Smith et al., 2020), a coarse resolution, fast running  
 129 AOGCM, which has been used in long-palaeo simulations (R. S. Smith, 2012; J. Gregory  
 130 et al., 2012; Roberts et al., 2014; Dentith et al., 2019; L. J. Gregoire et al., 2012) and  
 131 uncertainty quantification (L. Gregoire et al., 2010), coupled to the Glimmer Ice Sheet  
 132 model by downscaling SMB calculations (R. S. Smith et al., 2020), rather than previ-  
 133 ous work using a PDD SMB scheme (J. Gregory et al., 2012). This coupled model has  
 134 been used to simulate present and future Greenland Ice Sheet evolution (J. M. Gregory  
 135 et al., 2020). We start the manuscript by presenting the first attempt at simulating the  
 136 LGM with the FAMOUS-ice model with interactive ice sheets in Greenland and North  
 137 America. Here, we use an atmosphere-only version of FAMOUS, prescribing Sea Sur-  
 138 face Temperatures (SSTs) and Sea Ice Concentrations (SICs) in order to minimise bi-  
 139 ases in surface climate. We found that with the standard tuning that reproduced the mod-  
 140 ern Greenland shape and size (R. S. Smith et al., 2020) the model produces a collapse  
 141 of the North American ice sheet under LGM climatic conditions. We then present the  
 142 efficient method we developed to generate large ensembles of coupled climate ice sheet  
 143 simulations simultaneously varying uncertain parameters controlling the climate, ice sheet  
 144 and surface mass balance. Finally we show that albedo parameters are the primary con-  
 145 trol on uncertainty in our ensemble and we investigate the link between, cloudiness, albedo  
 146 and surface mass balance under modern and glacial conditions.

## 147 2 Model description and setup

148 FAMOUS-ice is a fast climate model coupled to the Glimmer ice sheet model (R. S. Smith  
 149 et al., 2020). The atmospheric component is that of FAMOUS, a fast low resolution gen-  
 150 eral circulation model designed for running simulations of the climate on multi-millennial  
 151 timescales (e.g. Dentith et al., 2019; L. J. Gregoire et al., 2012) and large ensembles for  
 152 calibration or uncertainty quantification purposes (L. Gregoire et al., 2010). The Glim-  
 153 mer ice sheet model is a fast simplified 3D dynamical ice sheet model based on the shal-  
 154 low ice approximation that is used to simulate continental ice sheets over glacial inter-  
 155 glacial cycles (L. J. Gregoire et al., 2015; Rutt et al., 2009). A multilayer surface snow  
 156 scheme is used in the atmosphere model to calculate surface mass balance (SMB) at ten  
 157 different elevation levels within each grid cell that contains part of an ice sheet. The SMB  
 158 calculated by the atmosphere model is regridded from the coarse FAMOUS-ice grid ( $7.5^\circ$ longitude  
 159 by  $5^\circ$ latitude) onto the surface of the Glimmer ice sheet model (in this case  $40km \times 40km$ )  
 160 each model year. The use of ten elevation levels on which SMB is calculated provides  
 161 a mean to effectively “downscale” the SMB from the coarse atmospheric grid to the finer  
 162 ice sheet grid. Coupled climate-ice sheet simulations would usually be too computationally  
 163 expensive to run as part of large multi-millennial ensembles, but the speed of both  
 164 FAMOUS and Glimmer make these experiments possible.

165 During the development of FAMOUS-ice, albedo parameters were manually tuned  
 166 to simulate a stable Greenland ice sheet at present day (R. S. Smith et al., 2020). The  
 167 model has been applied to evaluate the long-term future decline of the Greenland Ice Sheet  
 168 (J. M. Gregory et al., 2020). In both cases, sea surface temperatures and sea ice concen-  
 169 trations in FAMOUS were prescribed from the output of higher resolution and complex-  
 170 ity climate models to allow some control of the climate evolution and reduce the impact  
 171 of biases resulting from atmosphere-ocean and sea ice interactions. FAMOUS can also  
 172 be used with a dynamical ocean (e.g. Dentith et al., 2019) and the Glimmer ice sheet

173 component can be replaced with the more complex and computationally expensive BISI-  
174 CLES ice sheet model (Cornford et al., 2013; Matero et al., 2020; Gandy et al., 2018).

175 We setup FAMOUS-ice to simulate the climate of the Last Glacial Maximum, with  
176 interactive North American and Greenland ice sheets. We follow the PMIP4 LGM pro-  
177 tocol (Kageyama et al., 2017) to setup most of the climate boundary conditions, includ-  
178 ing the CO<sub>2</sub>, CH<sub>4</sub>, and N<sub>2</sub>O concentrations. Global orography and the land-sea mask  
179 was taken from the 21 ka BP Glac-1D reconstruction (Tarasov et al., 2012b), and prein-  
180 dustrial (PI) vegetation distribution was implemented and kept constant throughout the  
181 run. Thus our simulation neglect the effects of climate-ice-vegetation feedbacks that can  
182 affect ice sheet evolution (Stone & Lunt, 2013). The orbital configuration is set to 23  
183 ka BP, rather than 21 ka BP as in the PMIP4 protocol. This is 2,000 years prior to the  
184 ice sheet maximum extent to represent an orbit closer to point of maximum volume for  
185 the North American Ice Sheet (Peltier et al., 2015; Tarasov et al., 2012b). This slightly  
186 inhibits ice sheet growth as shown by a sensitivity experiment included in the suppl-  
187 ementary information.

188 SSTs and sea ice concentrations are taken from the statistical reconstruction of Astfalck  
189 et al. (2021), combining information from the PMIP LGM multi-model ensemble (Kageyama,  
190 Harrison, et al., 2021) and compilations of proxy data (Kucera et al., 2005), and their  
191 associated uncertainties. The method is able to generate ensembles of plausible SST and  
192 SIC pairs that can be used to drive atmosphere models. The simulated SSTs are in good  
193 agreement with the proxy-based reconstruction of Paul et al. (2021) with significantly  
194 warmer tropical SSTs than the data assimilation product of Tierney et al. (2020).

195 The interactive ice sheet model domain is set to cover North America, Greenland,  
196 and Iceland. All other ice sheets are fixed to match the Glac-1D reconstruction. The Glim-  
197 mer initial condition is taken from a previous ensemble of North American Ice Sheet deglacia-  
198 tions (L. J. Gregoire et al., 2016); specifically, ensemble member *Cano3-022* at 18.2 ka  
199 BP. This was chosen to represent an intermediate sized ice sheet resembling the likely  
200 extent during Marine Isotope Stage 3 (Gowan et al., 2021), from which to grow the North  
201 American ice sheet to an equilibrium ice sheet volume. In FAMOUS-ice, ice is able to  
202 grow by flowing onto a gridcell not previously covered in ice, but ice is not able to form  
203 from the accumulation of snow into an unglaciated gridcell. We thus chose an initial con-  
204 dition with a Cordilleran ice sheet. We also chose to start with ice already covering the  
205 Hudson Bay as the Glimmer ice sheet model does not represent the complex processes  
206 of grounding line migration. Simulations are run with 10 × ice sheet acceleration; i.e.,  
207 for every climate year simulated, Glimmer integrates for 10 ice sheet years with the same  
208 surface mass balance inputs (from the climate model). After this, the new Glimmer ice  
209 sheet surface elevation is passed back to the climate model, regridded and processed to  
210 update its orography and ice fraction fields.

211 We first run an initial standard experiment, using the atmosphere model param-  
212 eters from simulations that produce a stable contemporary Greenland ice sheet (J. M. Gre-  
213 gory et al., 2020) (apart from boundary conditions altered according to the PMIP4 LGM  
214 protocol), and ice sheet model parameters from previous simulations of the North Amer-  
215 ican ice sheet with glimmer (L. J. Gregoire et al., 2016). Parameters that may have an  
216 impact on the ice sheet evolution are listed in Table 1.

### 217 **3 Collapse of the LGM ice sheet with a standard setup**

218 Unexpectedly, with the the standard parameter values from (R. S. Smith et al., 2020),  
219 instead of growing from a mid-glacial ice sheet size, the North American ice sheet rapidly  
220 deglaciates in our standard experiment, losing half its volume in 2,500 years. This even-  
221 tually results in a simulation with LGM climate conditions, but no North American Ice  
222 Sheet (Figure 1). The deglaciation is driven by ablation across the North American Ice

**Table 1.** Key climate and ice sheet parameters in the simulation

Parameter	Standard Value	Ensemble Range	Units	Notes
Lapse rate	6	2-10	$K km^{-1}$	Prescribed lapse rate for air temperature used to downscale FAMOUS near-surface ice sheet climate onto surface elevation tiles. Downwelling longwave radiation is also adjusted for consistency
Daice	-0.35	-0.4-0	$K^{-1}$	Sensitivity of bare-ice albedo to surface air temperatures once the surface is in a melt regime
AVGR	0.007	0.001-0.01	$\mu m^{-1}$	Sensitivity of the snow albedo to variation in surface grain size
Fsnow	600	350-800	$kg m^{-3}$	The threshold in surface snow density at which the FAMOUS albedo scheme switches from a scattering paradigm appropriate for a conglomeration of snow grains to one more appropriate for a solid surface
Flow factor	3	1-10		The softness of ice. Increasing the factor makes the ice softer and more deformable
Mantle relaxation time	3000	500-9000	$yr$	The relaxation time of the mantle, a lower value essentially making the mantle less viscous, thus allowing a quicker topographic rebound.
Basal sliding	10	0.5-20	$mm yr^{-1}$ $Pa^{-1}$	The basal sliding rate. A higher value allows increased ice velocity.
RHCRIT	0.85	0.6-0.9		The threshold of relative humidity for cloud formation (R. Smith, 1990).
VF1	1.882	1-2	$ms^{-1}$	The precipitating ice fall-out speed (Heymsfield, 1977).
CT	0.000302	$5 \times 10^{-5}$ - $4 \times 10^{-4}$	$s^{-1}$	The conversion rate of cloud liquid water droplets to precipitation (R. Smith, 1990).
CW	0.001688	0.0001-0.002	$kg m^{-3}$	The threshold values of cloud liquid water for formation of precipitation (R. Smith, 1990). Only the value for the land is varied.
Entrainment rate	3	1.5-6		Entrainment rate coefficient Convection Scales rate of mixing between environmental air and convective plume.
Alpham	0.2152	0.2-0.65		The sea ice low albedo (Crossley & Roberts, 1995).

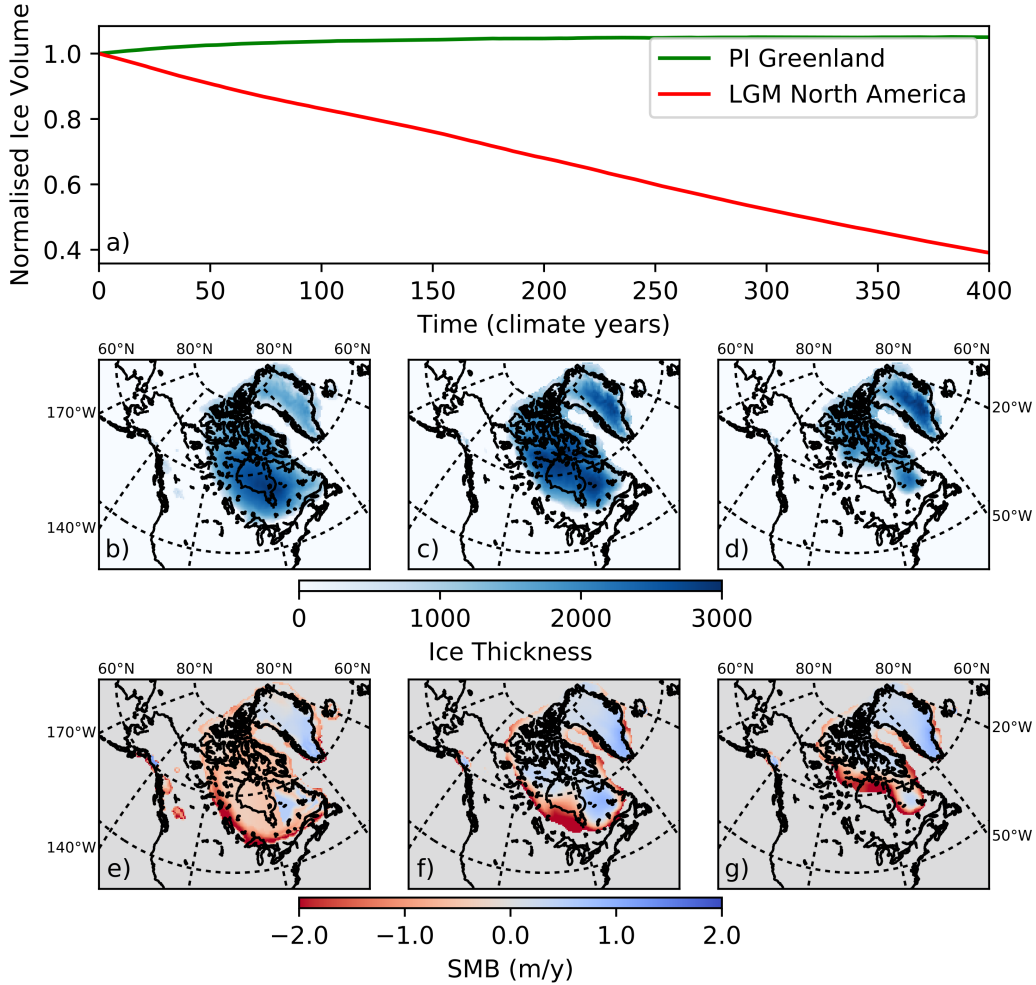


**Figure 1.** LGM North American Ice Sheet evolution in the standard setup. a) The ice sheet volume, normalised by the initial volume (green line) compared to the PI Greenland simulations (red line). b-d) Ice Thickness at 0, 2000 and 4000 years into the run. e-g) The SMB at 0, 2000 and 4000 years into the run.

223 Sheet, including the ice sheet interior (Figure 1e), which is present from the start of the  
 224 simulation and causes a rapid retreat of the southern margin northward through Hud-  
 225 son Bay (Figure 1b-d). The Greenland Ice Sheet on the other hand maintains its initial  
 226 extent, which corresponds to full glacial conditions, in good agreement with observations  
 227 (Simpson et al., 2009).

228 We know from geologic constraints (Dyke et al., 2002) that the ice sheet should be  
 229 considerably larger than simulated here (i.e. it should cover the whole of Canada). We  
 230 therefore conclude that parameters previously tuned to simulate the present day Green-  
 231 land ice sheet well (as in (R. S. Smith et al., 2020)) are not suitable for the LGM North  
 232 American Ice Sheet. To find a reasonable simulation, we thus need to fully explore the  
 233 uncertainty in model input parameters controlling the surface mass balance, ice sheet  
 234 dynamics and climatic conditions over the ice sheets in FAMOUS-ice as described be-

low, in essence to “de-tune” the model and find parameter combinations that produce good representations of the LGM North American Ice Sheet.

## 4 The Ensemble Approach

### 4.1 An Initial Pass: Wave 1

We started by running a large 280-member ensemble of simulations varying parameter values of Table 1. These values were sampled using  $k$ -extended Latin Hypercube sampling (Williamson, 2015) within ranges derived from previous uncertainty quantification work with FAMOUS (L. Gregoire et al., 2010) and Glimmer (L. J. Gregoire et al., 2016), with the addition of the Entrainment rate coefficient. We purposefully chose wide but plausible ranges (Table 1) with the aim to identify a region of the parameter space that would produce a reasonable North American ice extent at the LGM. We expected that similar to the standard simulation (Section 3), many runs would fully deglaciate. Thus, to optimise our use of computing resources, simulations were stopped at 2,500, 5,000, and 10,000 ice sheet years if they lost more than 25% of the initial ice sheet area.

In the majority of the 280 ensemble members, the North American ice volume reduces dramatically and thus all but 18 simulations were terminated early (figure 2a). However, five simulations remain relatively stable at the initial volume and area, and ice volume grows in twelve simulations. This deglaciation could be caused by errors in the simulated climate. We thus compared the ensemble results to prior simulations from PMIP3 and PMIP4 (Figure 3). We find that global mean temperature is broadly in line with previous PMIP3 and PMIP4 simulations - on the warmer end around 284K. The range of global mean temperatures in the ensemble is limited by the prescribed SSTs, which have a variability in the temperatures spatial distribution, but the same global mean SST (within 0.5K).

To assess our ice sheet results, we compare them to the ice extent reconstructed by Dyke et al. (2002). We calculate ice extent error as in Gregoire et al. (2016); by summing up the number of gridcells where the ice does not match the reconstruction. The maximum allowed error extent was chosen to align with the maximum LGM extent error from the NROY ensemble of L. J. Gregoire et al. (2016). L. J. Gregoire et al. (2016) applied a cumulative extent error over the whole deglaciation to identify their NROY set of simulations, we translated this into a maximum bound for our LGM extent error metric by applying our metric to their final NROY set and identifying the maximum value obtained. Constraints on North American ice volume are not as well known as ice extent, but can provide a useful metric for ruling out simulations. We chose to set a minimum threshold of  $2.1 \times 10^7 km^3$  for ice volume as in L. J. Gregoire et al. (2016), based on a variety of individual reconstructions (Clark & Tarasov, 2014; Lambeck et al., 2014; Peltier et al., 2015; Tarasov et al., 2012a). Only a small subset of the simulations (18 out of 280) terminate the simulation within this accepted criteria for volume and extent, highlighted by the green box in Figure 2b. We refer to the parameters of these simulations as Not Ruled Out Yet (NROY).

The average spatial extent of the ensemble is a poor fit to reconstructed ice extent (Figure 2c). Very few simulations approach the southern margin. In fact, despite stopping deglaciating simulations early only around 40% of simulations cover Hudson Bay, which should be in the ice sheet interior. Of the 18 simulations that do have a larger extent, there is a variety of ice configurations, but some consistent model-data mismatch. All the ice sheets that grow from the initial extent include extensive ice in Alaska, which was mostly ice free at the LGM (Dyke et al., 2002). After this first wave of 280 runs, more simulations were required to determine if these errors are systematic in the model set-up, or an artefact of the small number of simulations with a larger ice sheet volume.

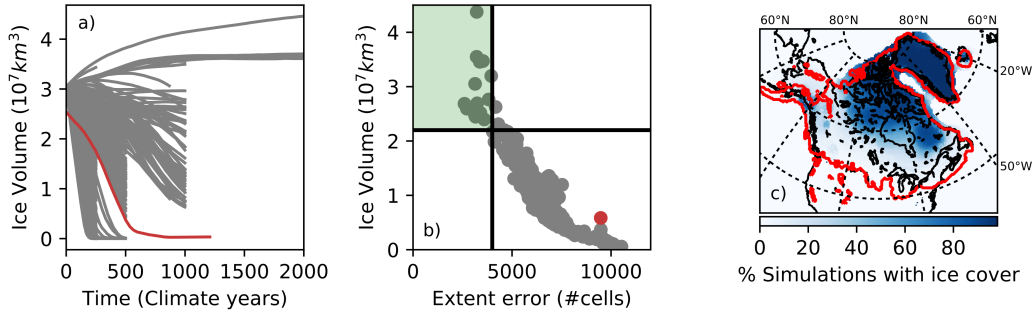


**Figure 2.** Wave 1 of the ensemble. a) North American Ice volume evolution for each ensemble member. b) The final ice volume and extent error (compared to the Dyke et al. (2002) margin) for each ensemble member. c) The % of simulations with ice cover compared to the Dyke et al. (2002) margin. The red line and point on panels a and b shows the control run, as shown in Figure 1.

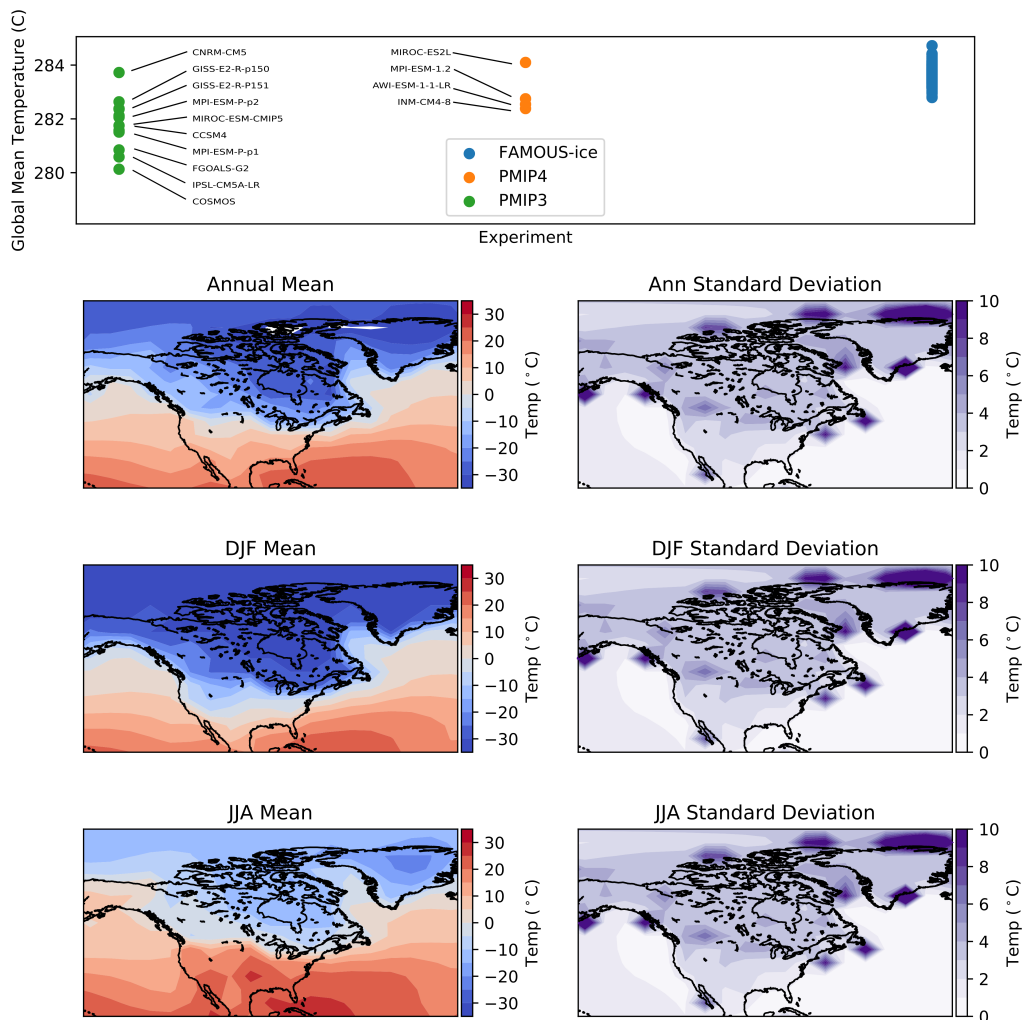


**Figure 3.** The surface temperature climatology of the Wave 1 ensemble compared to previous simulations as part of PMIP3 and PMIP4.

284

## 4.2 Refining the Ensemble: Wave 2

285

286

287

288

289

290

291

292

The fact that only 18 of 280 simulations in Wave 1 sustain a large enough North American ice sheet indicates that the majority of the parameter space, defined in Table 1, produce inappropriate conditions for the maintenance of a North American Ice Sheet. Searching through the parameter space to find realistic simulations thus required the use of statistical emulation and an intelligent and efficient iterative ensemble design to identify and target the space of ‘reasonable’ parameters. In order to provide optimal (parameter) space coverage of the design, whilst respecting the simulations that are already run, we use a stratified k-extended Latin Hypercube design (details follow).

293

294

295

296

297

298

299

300

301

302

Reaching an equilibrium in ice volume requires long simulations, particularly for the good simulations that take 10,000 years to reach a reasonable ice volume (Figure 4). In order to reduce computational cost, we investigated if it was possible to guess whether a simulation would be good or bad based on information from the start of the simulation. For the ice sheet to grow to a glacial maximum volume, it needs to accumulate more snow than the snow and ice lost in the ablation zone. In other words, the surface mass balance (SMB) at least needs to be positive. This is a conservative minimum requirement; in reality an ice sheet with a positive SMB may not reach the target reconstructed LGM extent, but this requirement excludes simulations that certainly cannot reach the target extent.

303

304

305

306

307

308

309

310

311

312

313

314

315

316

To efficiently select inputs for Wave 2 we generate a candidate set of runs by first identifying, from Wave 1, initial SMB values that result in plausible equilibrium ice-sheet areas; and second, emulating these initial SMB values as a function of the input parameters. We identified a strong relationship between the equilibrium ice-sheet area and the average SMB value from the first 20 years. Denote by  $b$  the 20 year averaged SMB value, and by  $A$  the “equilibrium” ice-sheet area after 10,000 ice sheet years. A predictive model of equilibrium ice-sheet area takes the form  $A = f(b) + \epsilon$  where  $f(\cdot)$  may be any function. We considered  $f$  to be either linear or a Gaussian process and found that the linear model gave more conservative in the uncertainty estimates, which was desired as we want the Wave 2 runs to bound the NROY space. Define a predictive interval  $P(b) = [f(b) + 3\sqrt{\text{var}(\epsilon)}, f(b) - 3\sqrt{\text{var}(\epsilon)}]$  from our predictive model. We target equilibrium ice-sheet areas in the interval  $T = [1.5 \times 10^7 \text{ km}^2, 2 \times 10^7 \text{ km}^2]$  and consider the  $b$  (and the corresponding input parameters) such that the intersection  $P(b) \cap T$  is non-zero as plausible for design in Wave 2.

317

318

319

320

321

322

323

324

325

326

327

328

To find combinations of input parameters that produce plausible values of  $b$  (and hence equilibrium ice-sheet areas), we ran three sub-waves of 20 year-long simulations to obtain the average SMB in the first 20 years. Note that simulations in the first sub-wave were run for 50 years to examine relationships other than 20-year SMB average that, in the end, were not used. Running these shorter simulations is still somewhat costly, and so we utilised a Gaussian Process (GP) emulator to design for parameterisations that was likely to produce desirable values for  $b$ . Define by  $x$  the multivariate vector of parameters that we build the emulator over: here  $x$  comprised of the 4 most influential parameters `FSNOW`, `AVGR`, `DAICE`, and `FLOW FACTOR` (see Table 1). We model  $b$  via a stochastic GP,  $b \sim \mathcal{GP}(x)$ , where the effects of the parameters not explicitly represented in  $x$  is handled by the stochasticity of the process. The specific set-up of this GP is provided in code as supplementary material.

329

330

331

332

333

334

335

From our three sub-waves of 20-50 year-long simulations, we are able to extract a candidate set of simulations for the Wave 2 ensemble. The first sub-wave (Wave 1.1) samples 200 ensemble members, which are predicted from the emulator to have non-negligible probability of positive SMB. This results in around 50% of simulations in this subwave having a positive SMB, an increase from 15% in the original wave (Figure 4b, Wave 1.1). We attempt to refine the predictive bounds on the GP model twice more (Figures 4c-d, Wave 1.2 and 1.3), with no improvement. This is likely due to the inherent stochas-

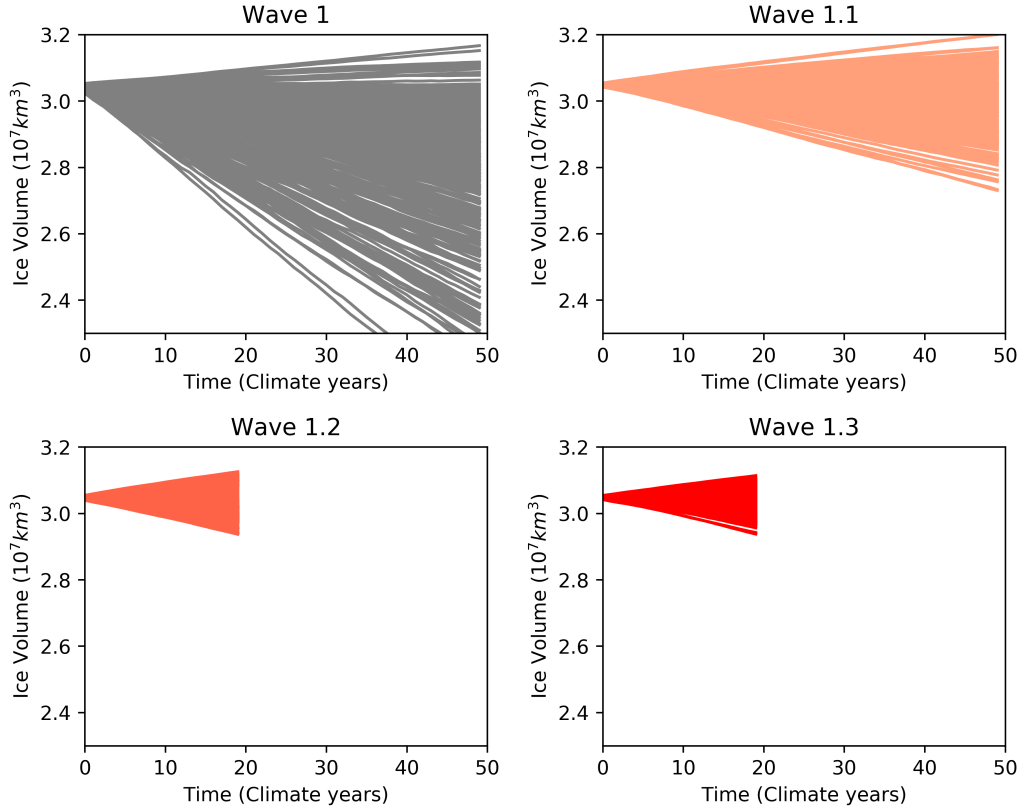


**Figure 4.** Ice Volumes simulated in the successive ensemble subwaves of simulations sampled to have a positive initial surface mass balance using the Gaussian Process emulator.

336 ticity of the climate model and cumulative effects of the parameters that we absorb into  
 337 the predictive error term. At the end of this process of iterative short waves, our candi-  
 338 date set contains over 1000 20-year long simulations that have a positive SMB over the  
 339 North American ice sheet. From this candidate set, we select an optimal (with respect  
 340 to space-filling and accounting for the previous Wave 1 runs) design of 200 ensemble mem-  
 341 bers to continue for a full 10,000 years to an equilibrium North American Ice Sheet. These  
 342 200 simulations make up our Wave 2. For context, this process of GP model subwaves  
 343 saved around 230,000 core hours (or about 2 months of real time) compared to running  
 344 a full second ensemble wave.

### 345 4.3 Wave 2 Results

346 By sampling a second wave of long simulation from the shorter subwaves, we de-  
 347 sign an ensemble of simulations that produce more NROY ice sheet extents, with 120/200  
 348 simulations maintaining or growing volume beyond the initial extent (Figure 5a). 176  
 349 more simulations out of the 200 wave 2 simulation are considered to be NROY based on  
 350 the volume and extent error thresholds previously described (Figure 5b), a factor of ten  
 351 increase from the 18 out of 280 simulations in Wave 1. This demonstrates the success  
 352 of our approach in efficiently identifying good combinations of parameters values. Some  
 353 simulations (56/200) shrank in volume slightly, but expended in area to meet both the  
 354 volume and area constraints to be considered NROY. The definition of an NROY en-  
 355 semble member is lenient, but could be further constrained (for example, by adding a

356 target for the top of the atmosphere energy balance) depending on future research ques-  
 357 tions or aims.

358 The mean ice sheet extent of the second wave is close to the southern ice sheet mar-  
 359 gin (Figure 5c). However, simulations that meet this margin still show some consistent  
 360 model-data mismatch. All simulations with a low Laurentide Ice Sheet extent error have  
 361 ice that is too extensive in Alaska. This is also common in ice sheet-only simulations with  
 362 Glimmer (L. J. Gregoire et al., 2016; Ji et al., 2021) driven by climate forcing from FA-  
 363 MOUS and from the higher resolution CCSM3 model, so is likely a systematic bias re-  
 364 sulting from the climate model. Alaskan ice extent was limited by the wider ice sheet  
 365 disrupting atmospheric circulations (Löfverström & Liakka, 2016; Tulenko et al., 2020).  
 366 The likelihood of matching observations is not helped by the climate coupling; a low res-  
 367 olution of FAMOUS struggles to simulate the temperature and precipitation gradients  
 368 caused by steep topography such as the Aleutian Range (Abe-Ouchi et al., 2007). Pre-  
 369 scribing the SMB forcing in an uncoupled model nudges the simulated ice sheets towards  
 370 the ice sheet prescribed (usually from reconstructions) in the climate-only model, encour-  
 371 aging a better match between modelled and reconstructed ice geometry, but not neces-  
 372 sarily for predictive reasons. Instead, in this case, a coupled climate-ice sheet model es-  
 373 sentially introduces additional freedom into the simulations to produce a greater vari-  
 374 ety of ice sheets.

375 At this point, we could repeat the subwave emulation step from the first wave of  
 376 simulations in an attempt to further narrow the parameter range and produce a third  
 377 wave of simulations with a greater proportion of NROY simulations. However, this sec-  
 378 ond wave has already produced 176 more NROY simulations, and running large waves  
 379 of simulations is computationally costly. We deem that there would be diminishing ben-  
 380 efits to running subsequent waves of simulations beyond this point.

## 381 5 Importance of Albedo Values

382 While 13 parameters are varied in the ensemble, it is clear that only three to four  
 383 of these parameters explain the majority of the variation in the model outputs. This is  
 384 demonstrated in Figure 6, where the parameter ranges for Wave 1 and Wave 2 are com-  
 385 pared. In Wave 2, the statistical emulator has removed regions of the parameter space  
 386 that do not produce reasonable ice sheet extents. There are large changes to the ranges  
 387 of FSNOW, DAICE, and AVGR, in the NROY ensemble, but limited changes for the other  
 388 ten parameters.

389 The parameters that are most influential on the simulated ice sheet volume all con-  
 390 trol the ice sheet surface albedo, these are the snow-ice density threshold (FSNOW), the  
 391 maximum albedo of bare ice (DAICE), and the snow grain size (AVGR) (Table 1, see  
 392 Smith et al 2020 for full details of how these terms are used in their respective param-  
 393 eterisations). As expected, the largest ice volumes result from having more reflective snow  
 394 and bare ice (from AVGR and DAICE respectively), and a high density threshold (FS-  
 395 NOW) to start considering snow to be ice (keeping a surface classed as more reflective  
 396 snow, rather than ice, for longer). The average surface albedo of the NROY simulations  
 397 is 0.1 higher than from the ruled-out simulations (Figure 5).

### 398 5.1 Why does the ice sheet deglaciate at low albedos?

399 We have shown that albedo parameters that have been manually tuned to produce  
 400 a reasonable contemporary Greenland ice sheet (J. M. Gregory et al., 2020; R. S. Smith  
 401 et al., 2020) produce a collapsed North American Ice Sheet at the LGM. Here, we ex-  
 402 plore the reasons why the present day Greenland ice sheet may not be a sufficient tar-  
 403 get for calibrating a coupled climate-ice sheet model. The contrasting behaviour between  
 404 present day Greenland and North American LGM ice sheets is associated with differ-

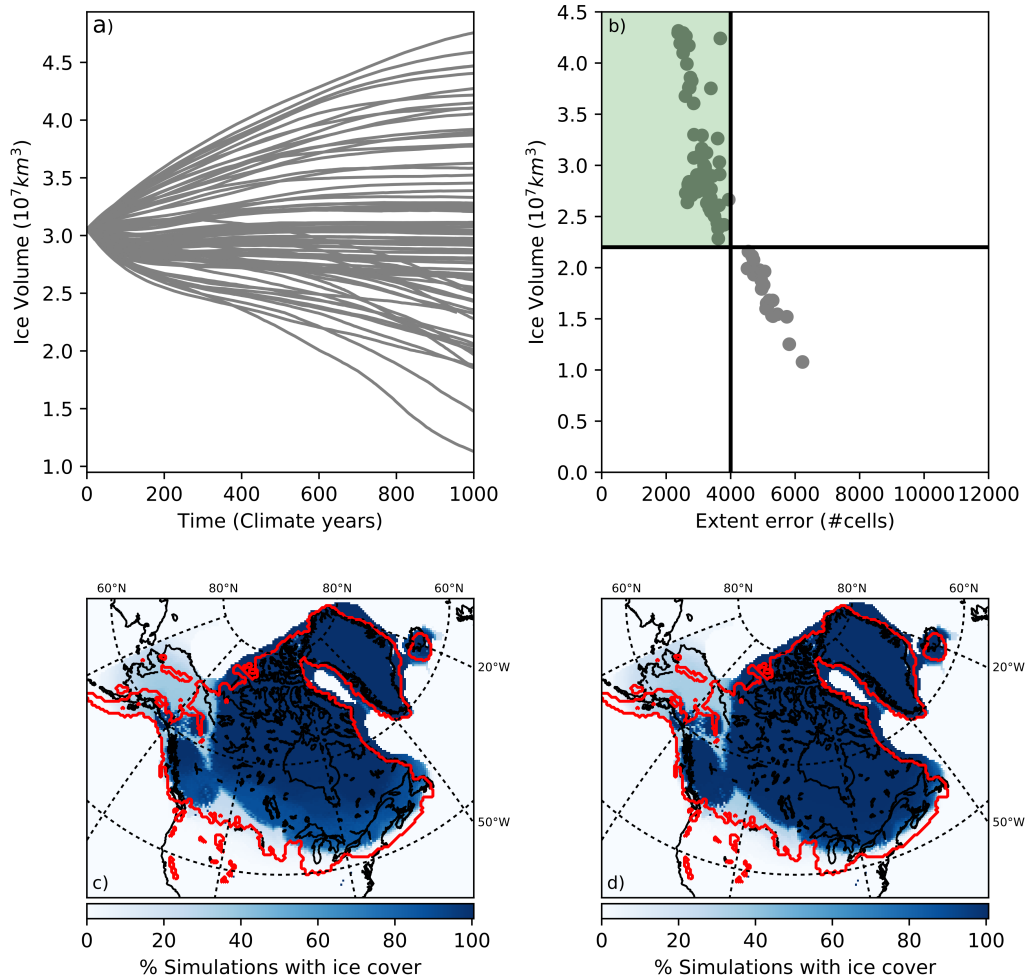


**Figure 5.** Wave 2 of the ensemble. a) Ice volume evolution for each ensemble member. b) The final ice volume and extent error (compared to the Dyke et al. (2002) margin) for each ensemble member. The % of simulations with ice cover shown as shades of blue compared to the Dyke et al. (2002) margin plotted as the red contour for the whole Wave 2 ensemble (c), and just for the NROY members of the Wave 2 ensemble (d).

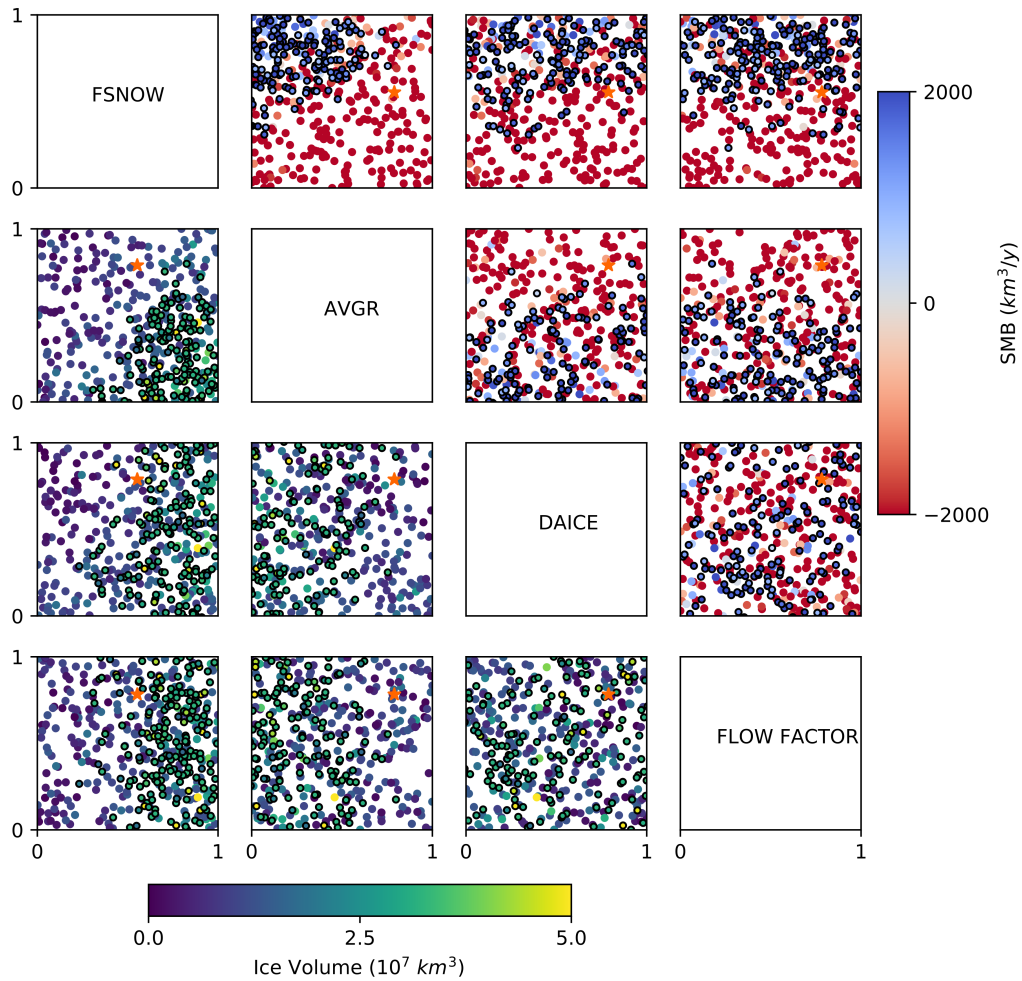


**Figure 6.** The resulting initial 20-year SMB and equilibrium Ice Volumes as a function of normalised albedo and flow factor parameter combinations in the ensembles. Wave 2 ensemble members are circled in black, and are clustered in the parameter space as a result of the GP emulator aiming for a positive SMB. For reference, the control simulation is marked by an orange star.

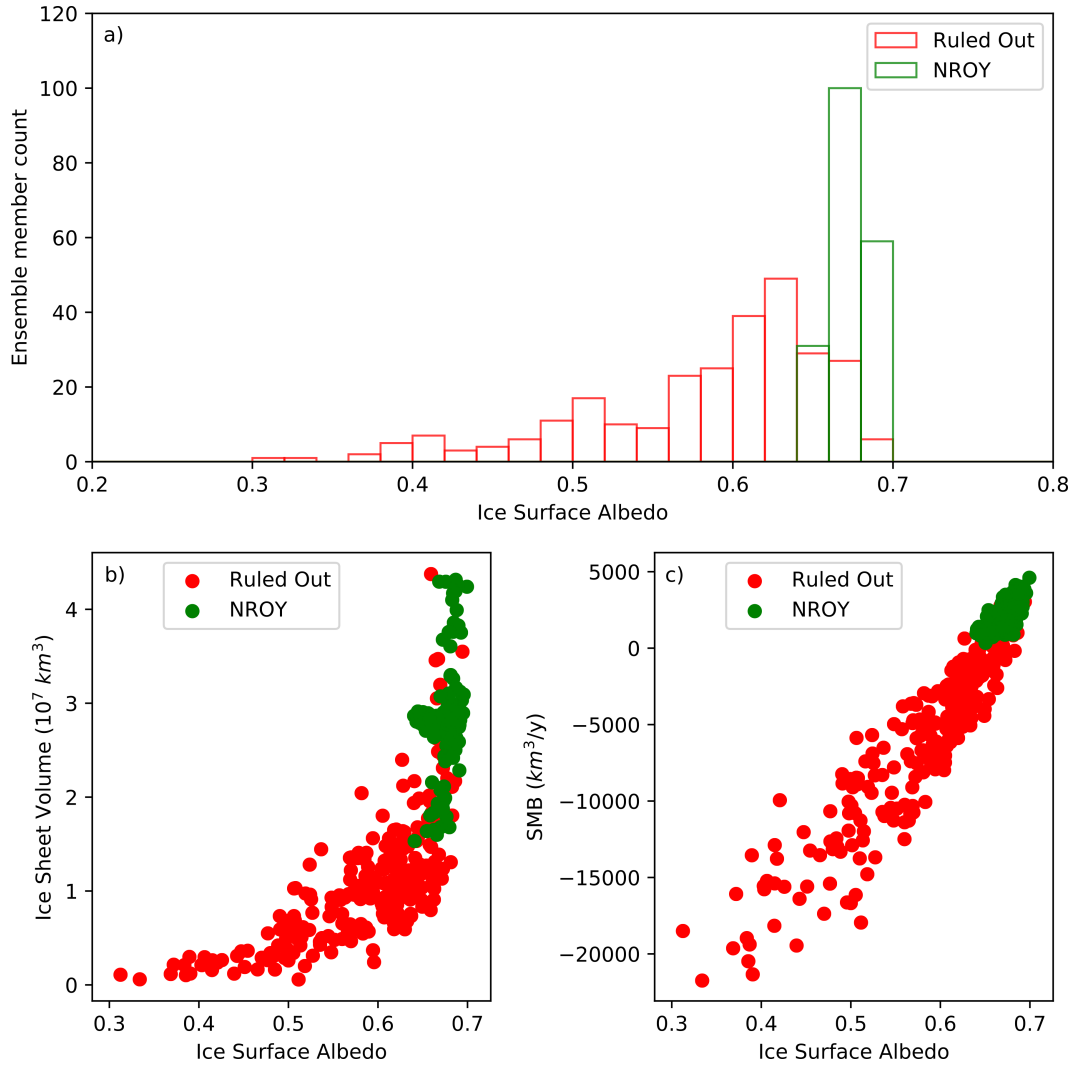


**Figure 7.** Average Ice Sheet surface albedos for NROY and Ruled Out ensemble members across both Wave 1 and Wave 2. a) The distribution of ice surface albedos for NROY and Ruled Out ensemble members. b) The relationship between final ice sheet volume and the ice sheet surface albedo. c) The relationship between the 30-year ice sheet SMB and the ice sheet surface albedo. All ice sheet surface albedos are taken as a 30-year average of the July albedo at the start of a simulations, so that ice sheet extents are comparable between ensemble members.

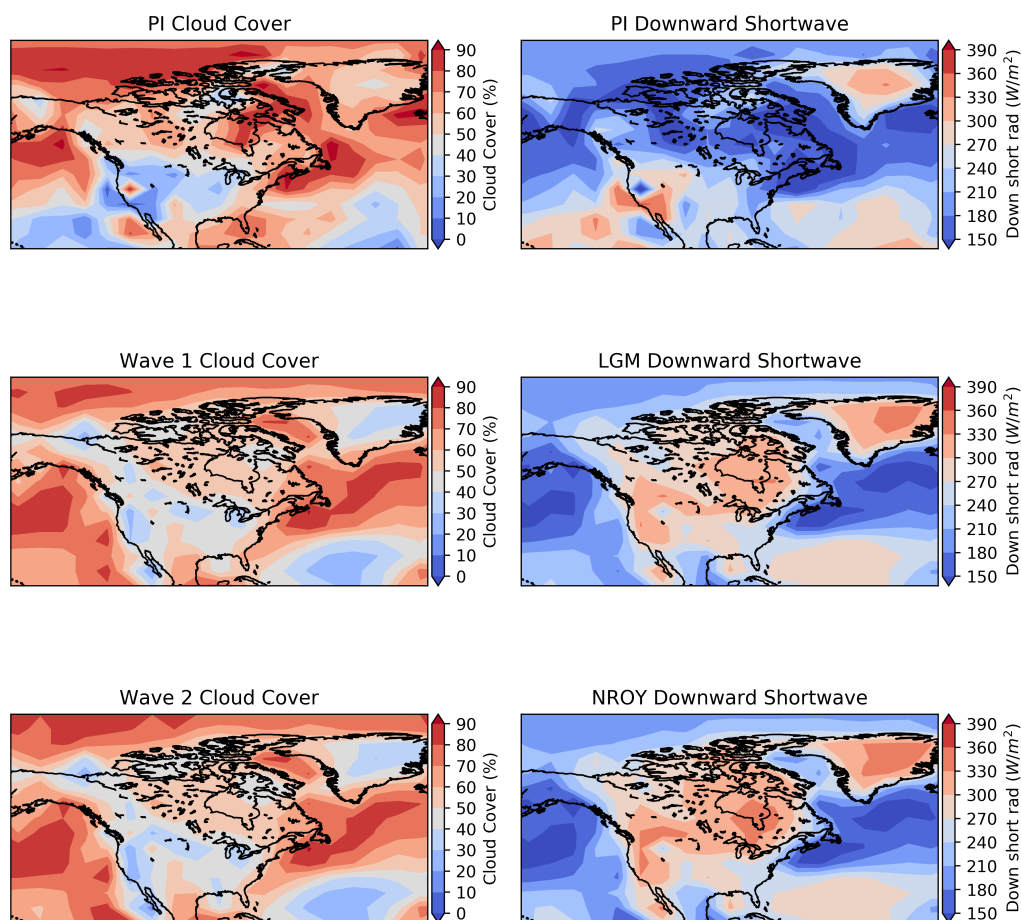


**Figure 8.** July cloud cover and downward shortwave radiation for the PI simulation, Wave 1, and Wave 2.

405 ences in the magnitude of downward shortwave radiation at surface and cloud cover be-  
 406 tween the two ice sheets. In the modern Greenland simulations, the ablation zone at the  
 407 ice sheet margin is often covered by thick clouds (Figure 8).

408 Simply, the relationship between cloud and ice sheet surface albedo can be split into  
 409 three groups (Figure 9). At high surface elevations there is lower temperatures and cloud  
 410 cover; a “sunny cold” regime that can sustain an ice sheet. At lower elevations there can  
 411 be sufficient cloud cover to reduce downward shortwave radiation, and therefore limit  
 412 ice sheet melt. In this “cloudy warm” regime the cloud cover means the ice sheet is in-  
 413 sensitive to its surface albedo. Finally, at lower elevations and limited cloud cover we can  
 414 see a “sunny warm” regime, where the ice sheet is highly sensitive to surface albedo pa-  
 415 rameters. Figure 9 shows downward shortwave radiation and ice surface albedo values  
 416 for each ice sheet surface gridbox in the control runs for PI Greenland and LGM North  
 417 America. While both runs occupy the “sunny cold” and “cloudy warm” regime, the “sunny  
 418 warm” regime is dominated by the LGM run. In this manner, the North American ice  
 419 sheet becomes very sensitive to low ice albedo parameters.

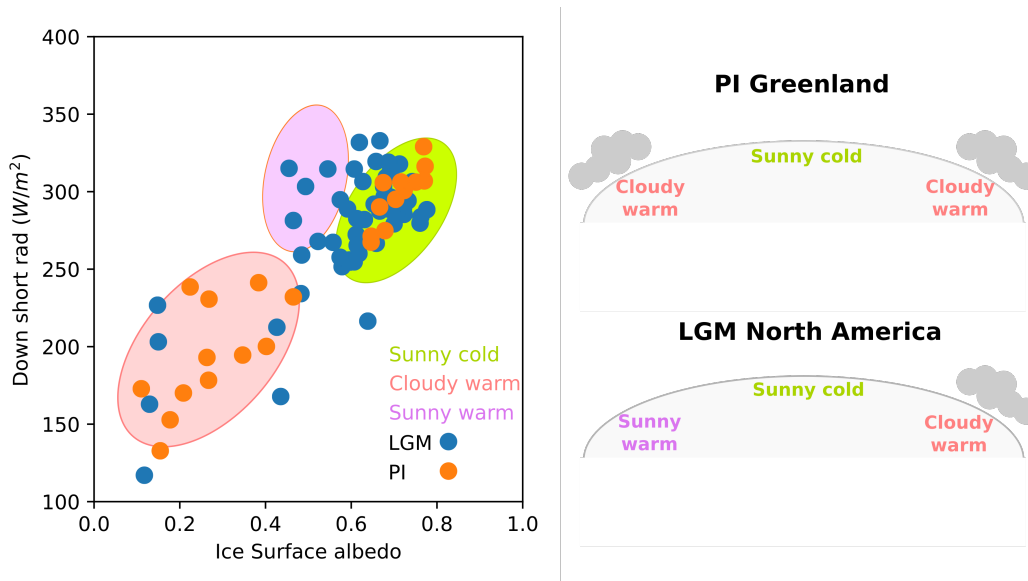


**Figure 9.** Comparison of energy balance between LGM North American and modern Greenland ice sheets: a) Downward Shortwave radiation vs ice surface albedo in each ice sheet gridcell for Greenland in the "standard" pre-industrial simulation (orange) and for the North American ice sheet in the "standard" LGM simulation (blue). Shaded ovals show the proposed surface albedo and radiation behaviour groups for the Greenland and Laurentide Ice Sheets. b) A schematic of the different radiative effect of clouds on the PI Greenland and LGM Laurentide Ice Sheets.

420 We further examine outputs from PMIP3 models (Brady et al., 2013; Voldoire et  
 421 al., 2013; Ullman et al., 2014; Sueyoshi et al., 2013; Adloff et al., 2018) to verify whether  
 422 the very strong downward shortwave radiation over the North American ice sheet ob-  
 423 served in FAMOUS-ice is a common feature among other models. The area-averaged val-  
 424 ues over the North American ice sheet are summarised in Table 2. The results show that  
 425 other PMIP models simulate stronger downward shortwave radiation at the southern mar-  
 426 gin of the ice sheet, and that FAMOUS-ice shows the smallest value for this together with  
 427 CCSM4 (Table 2). In other words, other models may impose an even stronger melt on  
 428 the ice sheet than in our simulations. This is associated with the strongest cloud radi-  
 429 ative effect in shortwave radiation in FAMOUS-ice and CCSM4. These results show that  
 430 the North American ice sheet would also be sensitive to low albedo values in other PMIP  
 431 models; if they allow a very small minimum bare ice albedo, a very large amount of solar  
 432 energy would be absorbed. Therefore, the larger sensitivity of the LGM North Amer-  
 433 ican ice sheet to low albedo parameters is likely not a unique feature of FAMOUS-ice,  
 434 but seems to be a common feature among other climate models.

435 There is a large uncertainty and variety in minimum ice sheet surface albedo among  
 436 PMIP models ranging from 0.2 in MRI and FAMOUS-ice to 0.7 in MPI (Alder & Hostetler,  
 437 2019). These differences in albedo values are induced by the combined effects of discrep-  
 438 ancies in the physics of the albedo scheme and biases in AGCMs. For the latter, biases  
 439 in cloud radiative effects (R. S. Smith et al., 2020) and horizontal resolution (Kapsch et  
 440 al., 2021) can affect the choice of albedo values. Importantly, the albedo values selected  
 441 are often strongly tuned to reproduce the modern SMB. This is sensible when the fo-  
 442 cus is on future change of Greenland ice sheet in the next few decades, since changes in  
 443 SMB are the dominant driver on this time scale. However, ice sheets evolve (e.g. in re-  
 444 sponse to climate) over much longer timeframes, and on a longer time-scale, when the

**Table 2.** Albedo and radiative characteristics of PMIP3 models and FAMOUS-ice. FAMOUS-ice values are taken from the Wave 2 ensemble, showing the mean value and ensemble range (in brackets).

PMIP3 Model	Surface albedo	Sfc down s/w radiation	Absorbed s/w at sfc
FAMOUS-ice	0.68 (0.56-0.75)	296 (265-324)	96 (71-126)
CCSM4	0.70	295.18	87.40
CNRM	0.34	307.67	204.47
GISS	0.66	341.52	116.34
IPSL	0.75	343.80	86.58
MIROC	0.75	351.76	86.51
MPI	0.83	348.92	58.07
MRI	0.57	318.19	138.25

445 ice sheet is subject to larger instabilities and more pronounced climate interactions, tun-  
 446 ing the albedo parameters may cause an unrealistic relationship between surface albedo  
 447 and cloud cover. Moreover, changes in the clouds over the next century could have pro-  
 448 nounced effects on SMB with unrealistic surface albedo.

449 In the case of FAMOUS-ice, the surface albedo parameters used for the contem-  
 450 porary Greenland ice sheet were originally tuned to a low value to compensate for an  
 451 excessive reflection of shortwave radiation by clouds (R. S. Smith et al., 2020). This was  
 452 performed to better simulate a stable and realistic Greenland ice sheet geometry under  
 453 modern day climate. However, the resulting ice albedo parameter sets are too low to pro-  
 454 duce a realistic North American ice sheet at the LGM due to the different cloud cover  
 455 and downward shortwave radiation over the ablation zone. Therefore we are in an un-  
 456 desirable situation where a model with good SMB in modern climate is unable to sim-  
 457 ulate the LGM North American Ice Sheets, and could also be unable to simulate other  
 458 ice sheets and time periods. This result suggests that overtuning the albedo to compen-  
 459 sate for biases in other components under modern climate may cause degraded simula-  
 460 tion results under different climate states, when the cloud properties and downward short-  
 461 wave radiation over ablation zones are different from modern. Most concerning, this sug-  
 462 gests that simulations projecting the future of the Greenland ice sheet are particularly  
 463 vulnerable to uncertain future cloudiness over the ice sheet.

## 464 6 Conclusions

465 We have applied a new coupled Climate-Ice Sheet model (FAMOUS-ice) to sim-  
 466 ulate the maximum extent of the last North American Ice Sheets. The standard model  
 467 setup manually tuned for modern day Greenland resulted in a collapsed ice sheet at the  
 468 LGM. We underwent a process of “detuning” the model, running hundreds of simula-  
 469 tions to produced a range of reasonable equilibrium ice sheets, enabling us to explore the  
 470 influence and importance of key uncertain parameters. Large parts of the parameter space  
 471 produced collapsed ice sheets at the LGM. Efficiently scanning the parameter space for  
 472 good input parameter combinations thus required an iteration of short simulations in-  
 473 formed by emulation of equilibrium ice volume as a function of initial surface mass bal-  
 474 ance. The results show that FAMOUS-ice is able to simulate the maximum extent of the  
 475 LGM North American Ice Sheet, with particularly good match to the southern Lauren-  
 476 tice limits, though some systematic ice overgrowth remains in Alaska.

477 From our results, we are able to identify that the parameters controlling ice sheet  
 478 surface albedo dominate the simulated variability in ice sheet geometry. Importantly, com-  
 479 binations of albedo parameter values that produced a reasonable contemporary Green-  
 480 land ice sheet do not necessarily produce a reasonable LGM North American Ice Sheet.  
 481 This is because albedo parameter can be overtuned to compensate for biases in modern  
 482 clouds over Greenland. The different cloud distribution over the Southern Laurentide  
 483 ice sheet at the Last Glacial Maximum provide a useful “stress test” for coupled climate-  
 484 ice sheet models. This highlights the potential problems of relying solely on contempo-  
 485 rary observations for model tuning. Efforts to find a region of the parameter space that  
 486 produce reasonable simulations of contemporary and glacial ice sheets are important, and  
 487 could lead to improved confidence in future ice sheet projections.

## 488 Author Contributions

489 Niall Gandy (principle researcher - climate ice sheet modelling): Methodology, Soft-  
 490 ware, Investigation, Formal Analysis, Data Curation, Writing - Original Draft, Visual-  
 491 ization. Lachlan Astfalck (co-researcher - statistics): Methodology, Software, Investiga-  
 492 tion, Formal Analysis, Writing - Original Draft. Lauren Gregoire (principle investiga-  
 493 tor): Conceptualization, Methodology, Writing - Review and Editing, Supervision, Project  
 494 Administration, Funding Acquisition. Ruza Ivanovic (co-investigator - climate modelling):  
 495 Conceptualization, Writing - Review and Editing, Supervision. Violet Patterson (con-  
 496 tributing researcher - 21 ka orbital simulation): Investigation. Sam Sherriff-Tadano (con-  
 497 tributing researcher - albedo and cloud analysis): Investigation, Formal analysis, Writ-  
 498 ing - Original Draft. Robin Smith (collaborator - climate-ice sheet modelling): Method-  
 499 ology, Software, Writing - Review and Editing. Daniel Williamson (co-investigator - statis-  
 500 tics): Methodology, Writing - Review and Editing, Supervision. Richard Rigby (software  
 501 scientist): Software.

## 502 Data Availability

503 Output from a Wave 2 simulation is archived online (10.17632/8kswwpnjyz.1). All  
 504 the other simulations can be accessed by contacting the author.

## 505 Acknowledgments

506 NG, LJG, LA, RFI, VLP, DW, and RR were funded by “SMB-Gen” UKRI Future Lead-  
 507 ers Fellowship MR/S016961/1. RFI, RSS and SST were funded by “RiSICMAP”, NERC  
 508 Standard Grant NE/T007443/1. This work was undertaken on ARC4, part of the High  
 509 Performance Computing Facilities at the University of Leeds.

## 510 References

- 511 Abe-Ouchi, A., Segawa, T., & Saito, F. (2007). Climatic conditions for modelling  
 512 the northern hemisphere ice sheets throughout the ice age cycle. *Climate of the*  
 513 *Past*, 3(3), 423–438.
- 514 Adloff, M., Reick, C. H., & Claussen, M. (2018). Earth system model simulations  
 515 show different feedback strengths of the terrestrial carbon cycle under glacial  
 516 and interglacial conditions. *Earth System Dynamics*, 9(2), 413–425.
- 517 Alder, J. R., & Hostetler, S. W. (2019). The dependence of hydroclimate projec-  
 518 tions in snow-dominated regions of the western united states on the choice  
 519 of statistically downscaled climate data. *Water Resources Research*, 55(3),  
 520 2279–2300.
- 521 Astfalck, L., Williamson, D., Gandy, N., Gregoire, L., & Ivanovic, R. (2021). Co-  
 522 exchangeable process modelling for uncertainty quantification in joint climate  
 523 reconstruction. *arXiv preprint arXiv:2111.12283*.

- 524 Brady, E. C., Otto-Bliesner, B. L., Kay, J. E., & Rosenbloom, N. (2013). Sensitivity  
525 to glacial forcing in the ccsm4. *Journal of Climate*, *26*(6), 1901–1925.
- 526 Clark, P. U., & Tarasov, L. (2014). Closing the sea level budget at the last glacial  
527 maximum. *Proceedings of the National Academy of Sciences*, *111*(45), 15861–  
528 15862.
- 529 Cornford, S. L., Martin, D. F., Graves, D. T., Ranken, D. F., Le Brocq, A. M.,  
530 Gladstone, R. M., . . . Lipscomb, W. H. (2013, jan). Adaptive mesh, finite vol-  
531 ume modeling of marine ice sheets. *Journal of Computational Physics*, *232*(1),  
532 529–549. Retrieved from [http://linkinghub.elsevier.com/retrieve/pii/  
533 S0021999112005050](http://linkinghub.elsevier.com/retrieve/pii/S0021999112005050) doi: 10.1016/j.jcp.2012.08.037
- 534 Crossley, J., & Roberts, D. (1995). Thermodynamic/dynamic sea-ice model. *Meteo-  
535 rological Office, Bracknell*.
- 536 Danabasoglu, G., Lamarque, J.-F., Bacmeister, J., Bailey, D., DuVivier, A., Ed-  
537 wards, J., . . . others (2020). The community earth system model version 2  
538 (cesm2). *Journal of Advances in Modeling Earth Systems*, *12*(2).
- 539 Davy, R., & Outten, S. (2020). The arctic surface climate in cmip6: status and de-  
540 velopments since cmip5. *Journal of Climate*, *33*(18), 8047–8068.
- 541 Dentith, J. E., Ivanovic, R. F., Gregoire, L. J., Tindall, J. C., & Smith, R. S. (2019).  
542 Ocean circulation drifts in multi-millennial climate simulations: the role of  
543 salinity corrections and climate feedbacks. *Climate Dynamics*, *52*(3), 1761–  
544 1781.
- 545 Dyke, A., Andrews, J., Clark, P., England, J., Miller, G., Shaw, J., & Veillette, J.  
546 (2002). The laurentide and innuitian ice sheets during the last glacial maxi-  
547 mum. *Quaternary Science Reviews*, *21*(1-3), 9–31.
- 548 Fettweis, X., Belleflamme, A., Erpicum, M., Franco, B., & Nicolay, S. (2011). *Esti-  
549 mation of the sea level rise by 2100 resulting from changes in the surface mass  
550 balance of the greenland ice sheet*. Intech, Croatia.
- 551 Franco, B., Fettweis, X., Lang, C., & Erpicum, M. (2012). Impact of spatial resolu-  
552 tion on the modelling of the greenland ice sheet surface mass balance between  
553 1990–2010, using the regional climate model mar. *The Cryosphere*, *6*(3),  
554 695–711.
- 555 Gandy, N., Gregoire, L. J., Ely, J. C., Clark, C. D., Hodgson, D. M., Lee, V., . . .  
556 Ivanovic, R. F. (2018, nov). Marine Ice Sheet Instability and Ice Shelf  
557 Buttressing Influenced Deglaciation of the Minch Ice Stream, Northwest  
558 Scotland. *The Cryosphere*, *12*(July), 1–24. Retrieved from [https://  
559 www.the-cryosphere.net/12/3635/2018/https://www.the-cryosphere  
560 -discuss.net/tc-2018-116/](https://www.the-cryosphere.net/12/3635/2018/https://www.the-cryosphere-discuss.net/tc-2018-116/) doi: 10.5194/tc-2018-116
- 561 Gandy, N., Gregoire, L. J., Ely, J. C., Cornford, S. L., Clark, C. D., & Hodg-  
562 son, D. M. (2021). Collapse of the last eurasian ice sheet in the north sea  
563 modulated by combined processes of ice flow, surface melt, and marine ice  
564 sheet instabilities. *Journal of Geophysical Research: Earth Surface*, *126*(4),  
565 e2020JF005755.
- 566 Ganopolski, A., Calov, R., & Claussen, M. (2010). Simulation of the last glacial cy-  
567 cle with a coupled climate ice-sheet model of intermediate complexity. *Climate  
568 of the Past*, *6*(2), 229–244.
- 569 Goelzer, H., Robinson, A., Seroussi, H., & Van De Wal, R. S. (2017). Recent  
570 progress in greenland ice sheet modelling. *Current climate change reports*,  
571 *3*(4), 291–302.
- 572 Gowan, E. J., Zhang, X., Khosravi, S., Rovere, A., Stocchi, P., Hughes, A. L., . . .  
573 Lohmann, G. (2021). A new global ice sheet reconstruction for the past 80 000  
574 years. *Nature communications*, *12*(1), 1–9.
- 575 Gregoire, L., Valdes, P., & Payne, T. (2010). Sensitivity of last glacial maximum ice  
576 sheet modelling to uncertainty in climate forcing. In *Egu general assembly con-  
577 ference abstracts* (p. 9492).
- 578 Gregoire, L. J., Otto-Bliesner, B., Valdes, P. J., & Ivanovic, R. (2016, sep). Abrupt

- 579 Bölling warming and ice saddle collapse contributions to the Meltwater  
 580 Pulse 1a rapid sea level rise. *Geophysical Research Letters*, *43*(17), 9130–  
 581 9137. Retrieved from <http://doi.wiley.com/10.1002/2016GL070356> doi:  
 582 10.1002/2016GL070356
- 583 Gregoire, L. J., Payne, A. J., & Valdes, P. J. (2012, jul). Deglacial rapid sea level  
 584 rises caused by ice-sheet saddle collapses. *Nature*, *487*(7406), 219–222. Re-  
 585 trieved from <http://www.nature.com/articles/nature11257> doi: 10.1038/  
 586 nature11257
- 587 Gregoire, L. J., Valdes, P. J., & Payne, A. J. (2015, nov). The relative contribution  
 588 of orbital forcing and greenhouse gases to the North American deglaciation.  
 589 *Geophysical Research Letters*, *42*(22), 9970–9979. Retrieved from [http://](http://doi.wiley.com/10.1002/2015GL066005)  
 590 [doi.wiley.com/10.1002/2015GL066005](http://doi.wiley.com/10.1002/2015GL066005) doi: 10.1002/2015GL066005
- 591 Gregory, J., Browne, O., Payne, A., Ridley, J., & Rutt, I. (2012). Modelling large-  
 592 scale ice-sheet–climate interactions following glacial inception. *Climate of the*  
 593 *Past*, *8*(5), 1565–1580.
- 594 Gregory, J. M., George, S. E., & Smith, R. S. (2020). Large and irreversible future  
 595 decline of the greenland ice sheet. *The Cryosphere*, *14*(12), 4299–4322.
- 596 Heymsfield, A. J. (1977). Precipitation development in stratiform ice clouds: A  
 597 microphysical and dynamical study. *Journal of Atmospheric Sciences*, *34*(2),  
 598 367–381.
- 599 IPCC. (2021). *Ocean, cryosphere and sea level change. in climate change 2021: The*  
 600 *physical science basis. contribution of working group i to the sixth assessment*  
 601 *report of the intergovernmental panel on climate change* [Book]. Cambridge,  
 602 United Kingdom and New York, NY, USA: Cambridge University Press. doi:  
 603 10.1017/9781009157896.011
- 604 Ivanovic, R., Gregoire, L., Kageyama, M., Roche, D., Valdes, P., Burke, A., ...  
 605 Tarasov, L. (2015). Transient climate simulations of the deglaciation 21–9  
 606 thousand years before present; pmip4 core experiment design and boundary  
 607 conditions. *Geoscientific Model Development Discussions*, *8*, 9045–9102.
- 608 Ji, W., Robel, A., Tziperman, E., & Yang, J. (2021). Laurentide ice saddle merg-  
 609 ers drive rapid sea level drops during glaciations. *Geophysical Research Letters*,  
 610 *48*(14), e2021GL094263.
- 611 Kageyama, M., Abe-Ouchi, A., Obase, T., Ramstein, G., & Valdes, P. (2021). Mod-  
 612 eling the climate of the last glacial maximum from pmip1 to pmip4. *Past*  
 613 *Global Changes Magazine*, *29*(2), 80–81.
- 614 Kageyama, M., Albani, S., Braconnot, P., Harrison, S. P., Hopcroft, P. O., Ivanovic,  
 615 R. F., ... others (2017). The pmip4 contribution to cmip6–part 4: Scientific  
 616 objectives and experimental design of the pmip4-cmip6 last glacial maximum  
 617 experiments and pmip4 sensitivity experiments. *Geoscientific Model Develop-*  
 618 *ment*, *10*(11), 4035–4055.
- 619 Kageyama, M., Harrison, S. P., Kapsch, M.-L., Lofverstrom, M., Lora, J. M., Miko-  
 620 lajewicz, U., ... others (2021). The PMIP4 Last Glacial Maximum exper-  
 621 iments: preliminary results and comparison with the PMIP3 simulations.  
 622 *Climate of the Past*, *17*(3), 1065–1089.
- 623 Kapsch, M.-L., Mikolajewicz, U., Ziemann, F. A., Rodehacke, C. B., & Schannwell, C.  
 624 (2021). Analysis of the surface mass balance for deglacial climate simulations.  
 625 *The Cryosphere*, *15*(2), 1131–1156.
- 626 Kucera, M., Rosell-Melé, A., Schneider, R., Waelbroeck, C., & Weinelt, M. (2005).  
 627 Multiproxy approach for the reconstruction of the glacial ocean surface  
 628 (margo). *Quaternary Science Reviews*, *24*(7-9), 813–819.
- 629 Lambeck, K., Rouby, H., Purcell, A., Sun, Y., & Sambridge, M. (2014). Sea level  
 630 and global ice volumes from the last glacial maximum to the holocene. *Pro-*  
 631 *ceedings of the National Academy of Sciences*, *111*(43), 15296–15303.
- 632 Löffverström, M., & Liakka, J. (2016). On the limited ice intrusion in alaska at the  
 633 lgm. *Geophysical Research Letters*, *43*(20), 11–030.

- 634 Matero, I. S., Gregoire, L. J., & Ivanovic, R. F. (2020). Simulating the early  
635 holocene demise of the laurentide ice sheet with bisicles (public trunk revi-  
636 sion 3298). *Geoscientific Model Development*, *13*(9), 4555–4577.
- 637 Menviel, L., Capron, E., Govin, A., Dutton, A., Tarasov, L., Abe-Ouchi, A., ... oth-  
638 ers (2019). The penultimate deglaciation: protocol for paleoclimate modelling  
639 intercomparison project (pmip) phase 4 transient numerical simulations be-  
640 tween 140 and 127 ka, version 1.0. *Geoscientific Model Development*, *12*(8),  
641 3649–3685.
- 642 Patton, H., Hubbard, A., Glasser, N. F., Bradwell, T., & Golledge, N. R. (2013, jul).  
643 The last Welsh Ice Cap: Part 2 - Dynamics of a topographically controlled  
644 icecap. *Boreas*, *42*(3), 491–510. Retrieved from [http://doi.wiley.com/  
645 10.1111/j.1502-3885.2012.00301.x](http://doi.wiley.com/10.1111/j.1502-3885.2012.00301.x) doi: 10.1111/j.1502-3885.2012.00301.x
- 646 Paul, A., Mulitza, S., Stein, R., & Werner, M. (2021). A global climatology of  
647 the ocean surface during the last glacial maximum mapped on a regular grid  
648 (glomap). *Climate of the Past*, *17*(2), 805–824.
- 649 Peltier, W. R., Argus, D., & Drummond, R. (2015). Space geodesy constrains ice  
650 age terminal deglaciation: The global ice-6g.c (vm5a) model. *Journal of Geo-  
651 physical Research: Solid Earth*, *120*(1), 450–487.
- 652 Roberts, W. H., Valdes, P. J., & Payne, A. J. (2014). Topography’s crucial role  
653 in heinrich events. *Proceedings of the National Academy of Sciences*, *111*(47),  
654 16688–16693.
- 655 Rutt, I. C., Hagdorn, M., Hulton, N., & Payne, A. (2009). The glimmer community  
656 ice sheet model. *Journal of Geophysical Research: Earth Surface*, *114*(F2).
- 657 Sellar, A. A., Jones, C. G., Mulcahy, J. P., Tang, Y., Yool, A., Wiltshire, A., ...  
658 others (2019). Ukesm1: Description and evaluation of the uk earth system  
659 model. *Journal of Advances in Modeling Earth Systems*, *11*(12), 4513–4558.
- 660 Shepherd, A., Ivins, E. R., A, G., Barletta, V. R., Bentley, M. J., Bettadpur, S.,  
661 ... Zwally, H. J. (2012, nov). A reconciled estimate of ice-sheet mass bal-  
662 ance. *Science (New York, N.Y.)*, *338*(6111), 1183–9. Retrieved from [http://  
663 www.ncbi.nlm.nih.gov/pubmed/23197528](http://www.ncbi.nlm.nih.gov/pubmed/23197528) doi: 10.1126/science.1228102
- 664 Simpson, M. J., Milne, G. A., Huybrechts, P., & Long, A. J. (2009). Calibrating  
665 a glaciological model of the greenland ice sheet from the last glacial maxi-  
666 mum to present-day using field observations of relative sea level and ice extent.  
667 *Quaternary Science Reviews*, *28*(17-18), 1631–1657.
- 668 Smith, R. (1990). A scheme for predicting layer clouds and their water content in a  
669 general circulation model. *Quarterly Journal of the Royal Meteorological Soci-  
670 ety*, *116*(492), 435–460.
- 671 Smith, R. S. (2012, feb). The FAMOUS climate model (versions XFXWB and  
672 XFHCC): description update to version XDBUA. *Geoscientific Model Develop-  
673 ment*, *5*(1), 269–276. Retrieved from [https://www.geosci-model-dev.net/  
674 5/269/2012/](https://www.geosci-model-dev.net/5/269/2012/) doi: 10.5194/gmd-5-269-2012
- 675 Smith, R. S., George, S., & Gregory, J. M. (2020). Famous version xotzb (famous-  
676 ice): a gcm capable of energy-and water-conserving coupling to an ice sheet  
677 model. *Geoscientific Model Development Discussions*, 1–25.
- 678 Smith, R. S., Mathiot, P., Siahaan, A., Lee, V., Cornford, S. L., Gregory, J. M., ...  
679 others (2021). Coupling the uk earth system model to dynamic models of the  
680 greenland and antarctic ice sheets. *Journal of Advances in Modeling Earth  
681 Systems*, *13*(10), e2021MS002520.
- 682 Stone, E. J., & Lunt, D. J. (2013). The role of vegetation feedbacks on greenland  
683 glaciation. *Climate dynamics*, *40*(11), 2671–2686.
- 684 Sueyoshi, T., Ohgaito, R., Yamamoto, A., Chikamoto, M., Hajima, T., Okajima, H.,  
685 ... others (2013). Set-up of the pmip3 paleoclimate experiments conducted  
686 using an earth system model, miroc-esm. *Geoscientific Model Development*,  
687 *6*(3), 819–836.
- 688 Tarasov, L., Dyke, A. S., Neal, R. M., & Peltier, W. (2012b, jan). A data-calibrated

- 689 distribution of deglacial chronologies for the North American ice complex from  
690 glaciological modeling. *Earth and Planetary Science Letters*, 315-316, 30–40.  
691 Retrieved from [https://www.sciencedirect.com/science/article/pii/](https://www.sciencedirect.com/science/article/pii/S0012821X11005243)  
692 S0012821X11005243 doi: 10.1016/J.EPSL.2011.09.010
- 693 Tarasov, L., Dyke, A. S., Neal, R. M., & Peltier, W. R. (2012a). A data-calibrated  
694 distribution of deglacial chronologies for the north american ice complex from  
695 glaciological modeling. *Earth and Planetary Science Letters*, 315, 30–40.
- 696 Tierney, J. E., Zhu, J., King, J., Malevich, S. B., Hakim, G. J., & Poulsen, C. J.  
697 (2020). Glacial cooling and climate sensitivity revisited. *Nature*, 584(7822),  
698 569–573.
- 699 Tulenko, J. P., Lofverstrom, M., & Briner, J. P. (2020). Ice sheet influence on atmo-  
700 spheric circulation explains the patterns of pleistocene alpine glacier records in  
701 north america. *Earth and Planetary Science Letters*, 534, 116115.
- 702 Ullman, D., LeGrande, A., Carlson, A. E., Anslow, F., & Licciardi, J. (2014). As-  
703 sessing the impact of laurentide ice sheet topography on glacial climate. *Cli-*  
704 *mate of the Past*, 10(2), 487–507.
- 705 Vernon, C. L., Bamber, J., Box, J., Van den Broeke, M., Fettweis, X., Hanna, E., &  
706 Huybrechts, P. (2013). Surface mass balance model intercomparison for the  
707 greenland ice sheet. *The Cryosphere*, 7(2), 599–614.
- 708 Vizcaíno, M., Lipscomb, W. H., Sacks, W. J., van Angelen, J. H., Wouters, B., &  
709 van den Broeke, M. R. (2013). Greenland surface mass balance as simulated  
710 by the community earth system model. part i: Model evaluation and 1850–  
711 2005 results. *Journal of climate*, 26(20), 7793–7812.
- 712 Voldoire, A., Sanchez-Gomez, E., Salas y Mélia, D., Decharme, B., Cassou, C.,  
713 Sénési, S., ... others (2013). The cnrm-cm5. 1 global climate model: descrip-  
714 tion and basic evaluation. *Climate dynamics*, 40(9), 2091–2121.
- 715 Williamson, D. (2015). Exploratory ensemble designs for environmental models us-  
716 ing k-extended latin hypercubes. *Environmetrics*, 26(4), 268–283.
- 717 Ziemen, F. A., Rodehacke, C. B., & Mikolajewicz, U. (2014, oct). Coupled ice  
718 sheet–climate modeling under glacial and pre-industrial boundary condi-  
719 tions. *Climate of the Past*, 10(5), 1817–1836. Retrieved from [https://](https://www.clim-past.net/10/1817/2014/)  
720 [www.clim-past.net/10/1817/2014/](https://www.clim-past.net/10/1817/2014/) doi: 10.5194/cp-10-1817-2014